

# PROPOSAL FOR EXPERIMENT AT LEPS BEAM LINE

September 26, 2005

## Performance of the spaghetti calorimeter with individual fiber readout

### SPOKES PERSON:

Toru Matsumura

*Department of Applied Physics, National Defense Academy, Yokosuka 238-8686*

position: Research Associate

e-mail: toru@nda.ac.jp

phone: 046-841-3814 (ex.3912)

### EXPERIMENTAL GROUP:

Name	Affiliation	Position
Toru Matsumura	National Defense Academy	Research Associate
Takao Shinkawa	National Defense Academy	Associated Professor
Tsuyoshi Tojo	National Defense Academy	Student (M1)
Taku Yamanaka	Osaka University	Professor
Mitsuhiro Yamaga	Osaka University	Research Associate
Eito Iwai	Osaka University	Student (M1)
Shun Kajiwara	Osaka University	Student (M1)
Yohei Kuroki	Osaka University	Student (B4)
Yorihito Sugaya	LNS, Osaka University	Research Associate

### RUNNING TIME:

- 1 day for the detector setup
- 2 days for the tuning ( circuit and colimator position )
- 4 days for the data taking

### BEAM:

- Collimated gas-bremsstrahlung beam (No Laser)

## Summary of the proposal

We propose an experiment to study the performance of the spaghetti calorimeter with individual fiber readout at LEPS/SPring-8. A prototype module of the spaghetti calorimeter, consisting of the grooved lead sheets and 12,000 pieces of scintillating fibers, was constructed as a part of R&D program for the  $K_L$  rare-decay experiment at J-PARC. The main purpose of the beam test is to check the performance of the shower-profile measurement by 2-dimensional imaging, and measure the energy, position and angular resolutions of the spaghetti calorimeter. The result obtained from the beam test will be utilized for new calorimeter design for the J-PARC experiment.

The prototype module will be placed between DC3 and TOF counters in the experimental hatch. The bremsstrahlung photon beam having an energy up to 8 GeV is injected on the module. The half of fibers which located in the upstream part of the module are read individually with a CCD camera for shower profile measurement.

To study the performance of the spaghetti calorimeter, we request 1 day for detector setup, 2 days for tuning of circuit and collimator position and 4 days for data taking. We will use the bremsstrahlung photons produced at the straight section in the storage ring; thus, no laser is needed. No material in the beam line is required except for the absorber for synchrotron radiation (Pb 1.5 mm) and drift chambers. Timing signals of the tagger hodoscope are necessary for linearity check and absolute energy calibration. Special request is that we need a collimator ( $< 1 \text{ mm}\phi$ ) just before the sweep magnet in the laser hatch.

# Contents

<b>1</b>	<b>Physics Motivation</b>	<b>4</b>
<b>2</b>	<b>Prototype spaghetti-calorimeter module</b>	<b>4</b>
2.1	Design . . . . .	4
2.2	Readout system for imaging . . . . .	6
2.3	Performance (simulation) . . . . .	8
2.4	Construction . . . . .	14
<b>3</b>	<b>Proposed Experiment</b>	<b>15</b>
3.1	General description of the experiment . . . . .	15
3.2	Beam condition . . . . .	15
3.3	Data Acquisition . . . . .	16
3.4	Data statistics . . . . .	17
<b>4</b>	<b>Conclusion and Requests</b>	<b>18</b>

# 1 Physics Motivation

The branching ratio of the  $K_L \rightarrow \pi^0 \nu \bar{\nu}$  decay is one of important observables because it is directly related to the parameter  $\eta$  which is sensitive to the direct CP violation. In the standard model, the  $Br(K_L \rightarrow \pi^0 \nu \bar{\nu})$  was predicted to be  $3 \times 10^{-11}$  within a few percent uncertainty. Therefore, the measurement of the branching ratio gives us a chance to hunt the signature of the beyond the standard model.

Experimental studies for determination of the branching ratio have been achieved by KTeV/FNAL and E391a/KEK, and the upper limit has been obtained  $Br(K_L \rightarrow \pi^0 \nu \bar{\nu}) < 3 \times 10^{-7}$  at the present time. In order to fix the branching ratio, better single-event sensitivity is required for the experiment, i.e. we need more  $K_L$ -beam intensity and less background events. Such an experiment has been proposed at J-PARC, where we expect to observe 100 events of the  $K_L \rightarrow \pi^0 \nu \bar{\nu}$  decay[1]. Since two neutrinos are included in the final state, the signal of the  $K_L \rightarrow \pi^0 \nu \bar{\nu}$  event is that there are signals of two photons, coming from  $\pi^0$  decay, on a electro-magnetic calorimeter and nothing other. Thus, a  $4\pi$  detector system with low detection inefficiency is required. We are planning to prepare a segmented crystal calorimeter for the end-cap part and a cylindrical veto counter for barrel part.

One of the serious background in the experiment would be  $K_L \rightarrow \pi^0 \pi^0$  decay, where the branching ratio is  $9.3 \times 10^{-4}$ . The reason is that if two photons coming from the  $K_L \rightarrow \pi^0 \pi^0$  decay are missing due to some reasons, the observed events satisfy the signal condition of the  $K_L \rightarrow \pi^0 \nu \bar{\nu}$  decay. There are two sources of the photon missing: inefficiency of the detector system and cluster fusion in the crystal calorimeter. The solution to reduce the cluster-fusion events is to install a position sensitive detector just in front of the end-cap crystals. The detector also has to work as a calorimeter. One of the possible candidate is a spaghetti calorimeter, consisting of a lot of scintillating fibers embedded in lead.

A prototype module of the spaghetti calorimeter was constructed as a part of R&D program for the  $K_L$  rare-decay experiment at J-PARC. The aim of the R&D is to check the performance of the spaghetti calorimeter using a photon beam. Thus, we planned to perform the beam test with high-energy photon-beam at LEPS/SPring-8.

## 2 Prototype spaghetti-calorimeter module

### 2.1 Design

In this beam test, we will employ the prototype spaghetti-calorimeter module, where the number of fiber layers is 160 layers (see Fig.1). Totally 12,000 single-clad scintillating-fibers (Kuraray

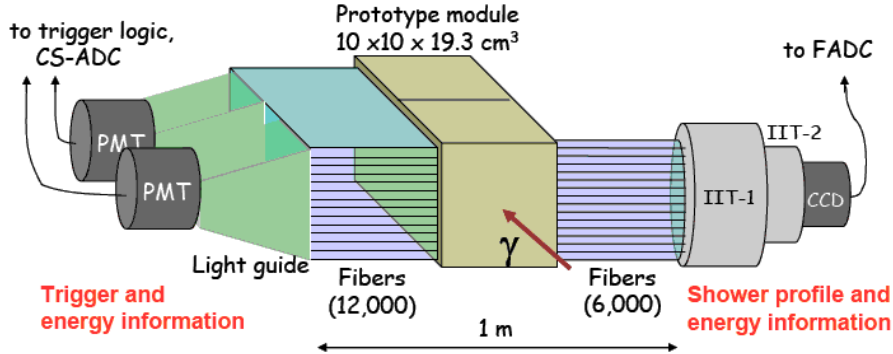


Figure 1: Components of the prototype spaghetti module.

SCSF-78, 1 mm $\phi$  diameter) are aligned parallel to the horizontal axis. The interval of between each fiber is 1.35 mm. The cross-sectional area of the module is 100  $\times$  100 mm<sup>2</sup>, and the length is 193 mm which corresponds to the 12.1 radiation lengths ( $X_0$ ). The length of each fiber is about 1 m, hence the distance from the center of the module to the both ends is about 0.5 m.

We divide this module into two parts: an upstream part and a downstream part. The upstream part is the first 80 fiber-layers from upstream to the beam ( $\sim 6X_0$ ). The image intensifier tube (IIT) is attached to the one end of the fiber bundle of the upstream part. Scintillation light coming from the fibers is amplified to  $\sim 10^7$  by IIT with keeping the 2-dimensional information, and then it is sent to a CCD camera for imaging. We refer this image-readout system as IIT-CCD system. Another end of the fiber bundles of the upstream part is connected to a photo-multiplier tube (PMT) via an acrylic light-guide, which is used to monitor the energy deposit in the upstream part. On the other hands, we do not read 2-dimensional image for the downstream part since it is impossible to read all scintillating fibers with one unit of IIT-CCD system. Thus, we only read one end of the fiber bundle with a PMT for the downstream part, and another end is kept free.

The light attenuation of the SCSF-78 was measured with a  $^{90}\text{Sr}$   $\beta$ -ray source, where the one end of the fiber was connected to a PMT (H7195). Here, average energy deposit of an electron passing through an fiber (1 mm $\phi$ ) was estimated to be 150 keV. Figure 2 shows the average number of photo-electrons ( $\overline{N_{p.e.}}$ ) as a function of the distance from the PMT. A double exponential function was fitted to the data, and the attenuation lengths were  $L_s = 44.3 \pm 1.4$  cm for a short component and  $L_l = 350 \pm 3$  cm for a long component, respectively. The distance from the center of the prototype PMT to the IIT surface is 50 cm; therefore,  $\overline{N_{p.e.}}$  for the fiber whose energy deposit is 150 keV is expected to be  $\overline{N_{p.e.}} \sim 6$  on the IIT.

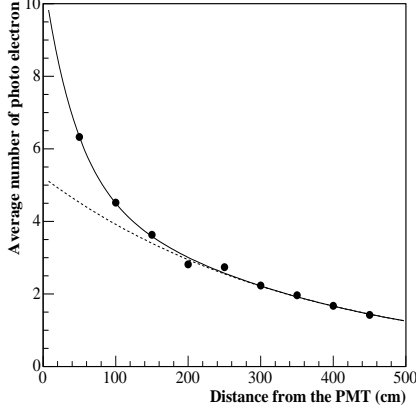


Figure 2: Attenuation curve of a SCSF-78 scintillating fiber. Solid line shows a double-exponential function fitted to the data. Dashed line shows its longer component.

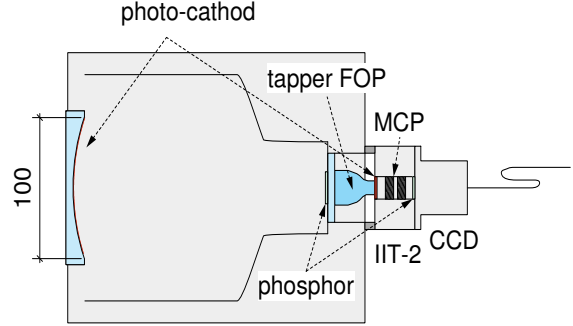


Figure 3: IIT-CCD system for imaging of the fiber-hits

## 2.2 Readout system for imaging

Information of the two-dimensional fiber-hits is collected with IIT-CCD system in order to reconstruct the shower profile produced by an incident photon. The system consists of the following parts:

- A large-diameter image intensifier (IIT-1)
- A tapered fiber-optic-plate (taper FOP)
- An image intensifier with 2-stages micro-channel plates (IIT-2)
- A CCD camera

An illustration of the IIT-CCD system is shown in Fig.3. The principle of the two-dimensional imaging is described below.

1. Scintillation lights are converted to photo-electrons at the photo-cathode of IIT-1 ( $Q.E. \sim 20\%$ ), which has a  $100\text{ mm}\phi$  entrance window consisting of a UV-transmitting FOP. The photo-electrons are focused with electric field onto the phosphor screen (P-11) at the end of IIT-1. Its diameter is 25 mm; hence, the imaging area reduces to  $1/16$  at the phosphor screen.

2. The phosphorescence lights produced at the end of IIT-1 are collected by the photo-cathode of IIT-2 via a taper FOP; photo electrons are regenerated again. In IIT-2, the photo-electrons are multiplied to  $\sim 10^6$  with the 2-stages of micro-channel-plate (MCP), and then they hit the phosphor screen (P-43) at the end of IIT-2.
3. The fiber image at the phosphor screen is recorded by a TV-rate CCD-camera located just after IIT-2. The analog signals from the CCD will be sent to a flash ADC module for digitization.

Detail of each component is described below.

**IIT-1** IIT-1 (HAMAMATSU V5502UX) is a large-diameter IIT, which has been used for CHORUS experiment at CERN. It has a 100 mm $\phi$  entrance-window and a 25 mm $\phi$  phosphor-screen at the end. Since IIT-1 has no micro-channel-plate, it basically works as an electronic lens to reduce the imaging area. However, because of high anode voltage (20 kV), photo-electrons are accelerated, and hence the number of photons produced at the phosphor screen is gained.  $\gamma/e$  ratio of the phosphor is defined as the number of photons produced by a photo-electron; it was about 300 for IIT-1 in the case of pulsed light.

**Taper FOP** A tapered fiber-optic-plate is set between IIT-1 and IIT-2 via silicone grease (C10000). The purpose is the image reduction of the output area of IIT-1 to the size of CCD camera. The entrance area of the FOP is 27 mm $\phi$  and the exit area is 10.8 mm $\phi$ , respectively. The length of the FOP is 34.5 mm.

**IIT-2** To measure the image whose light yield is the level of single photo-electron, we use a high sensitivity IIT (HAMAMATSU C9016-24MOD), which has 2 stages of MCP. The effective size of the photo-cathode is 17.5 mm $\phi$ . The output area is 12.8  $\times$  9.6 mm, which is the size that the light-yield uniformity is ensured by manufacturer. The photo-cathode of IIT-2 is made of multi-alkali materials, and the sensitive wave-length ranges 185 nm to 900 nm (maximum at 430 nm). Typical gain of IIT-2 is  $3.0 \times 10^6$ . In order to reduce S/N ratio, IIT-2 accepts gate signals.

**CCD camera** We employ HAMAMATSU C9018, which is an inter-line transfer CCD with FOP window, for an imaging device. The effective area of the CCD is 12.8(H) $\times$ 9.6(V) mm, and the number of pixels is 768(H) $\times$ 494(V), totally 0.38 Mpixels. Readout of the both even and odd fields is performed every 16.6 ms alternately; hence readout time for one frame is 33.3 ms.

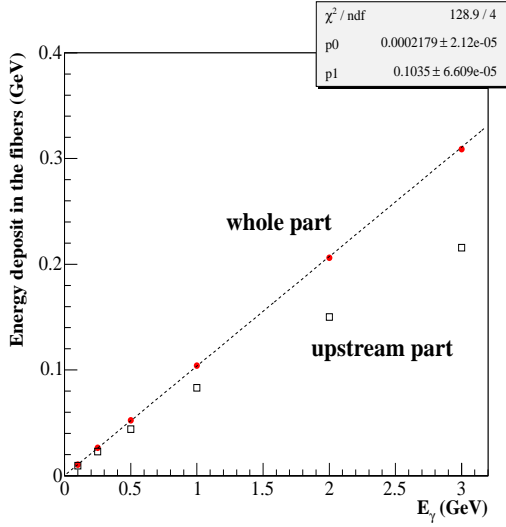


Figure 4:  $E_\gamma$  dependence of the energy deposit in the fiber region.

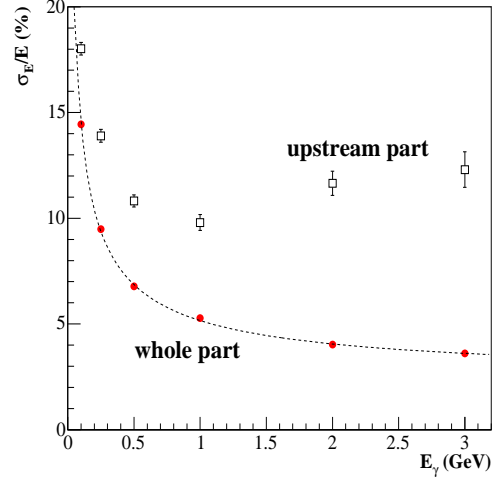


Figure 5: Energy resolution ( $\sigma_E/E$ ) as a function of  $E_\gamma$ .

### 2.3 Performance (simulation)

To evaluate the response of the prototype module, a simulation code which took into account all details of the components was developed using the Geant4 package[2] (version 6.1). The spaghetti module has a fine structure consisting of scintillating fibers, lead radiator and epoxy glue. In Geant4, the tracking of particles is done in finite step size. Although the calculation time becomes quite long, each step has to be set sufficiently small, compared to the distance between various boundaries to ensure proper energy-loss calculation. Here, we set the maximum step length and the cut-off range to 0.01 mm and 0.05 mm respectively. In this section, the performance of the prototype module will be discussed with this simulation code.

#### Visible ratio

Photon beams were injected on to the center of the module surface for various incident energy ( $E_\gamma$ ). Figure 4 shows the energy deposit in the fiber region for different incident energies. In this figure, the energy deposit in the whole part ( both upstream and downstream parts ) and fibers in the upstream part are plotted. For the whole part, the fraction of the energy deposit, which is referred as visible ratio, is independent of  $E_\gamma$ . The visible ratio was estimated to be 10.35% from the plot.

In contrast, for the upstream case, the energy deposit does not increase linearly as  $E_\gamma$  increases. The reason is that the detector length of the upstream part ( $\sim 6X_0$ ) is not enough to confine the shower particles, and hence the effect that the the position of shower maximum moves toward downstream side for higher  $E_\gamma$  is visible. Note that in this case the distribution of the energy deposit has low energy tail; thus, we estimated its mean value with a Gaussian plus exponential function:

$$F(x) = \begin{cases} A \exp -\frac{1}{2} \left( \frac{x - \mu}{\sigma} \right)^2 & x < x_j \\ A \exp -\frac{1}{2} \left( \frac{x_j - \mu}{\sigma} \right)^2 \exp \left( \frac{x_j - x}{a} \right) & x \geq x_j, \end{cases} \quad (1)$$

where  $\mu$  shows the mean value of the Gauss distribution,  $a$  indicates the slope parameter for the exponential function and  $x_j$  means a border between two functions.

### Energy resolution

The energy resolutions for both cases ( all parts and only upstream parts ) is shown in Fig.5 as a function of  $E_\gamma$ . Following function were fitted to the plot for total part,

$$\frac{\sigma_E}{E} = \sqrt{a^2 + \left( \frac{b}{\sqrt{E}} \right)^2}, \quad (2)$$

where  $a$  indicates the parameter that explains the shower-leakage effect,  $b$  is the parameter dominated by sampling fluctuation and  $E$  is incident energy in GeV. We obtained the parameters from the fitting, and these were  $a = 2.50 \pm 0.10\%$  and  $b = 4.52 \pm 0.04\%$ , respectively. Therefore, the energy resolution of the 1 GeV photons is  $\sigma_E/E = \sqrt{a^2 + b^2} = 5.16 \pm 0.06\%$ . Note that this resolution does not include the contribution from the fluctuation of the number of photo-electrons.  $\overline{N_{p.e.}}$  of the one fiber was measured as discussed in section 2.1, and it was  $\overline{N_{p.e.}} \sim 6$  for 150 keV energy deposit. The energy deposit for  $E_\gamma = 1$  GeV is 105 MeV from the visible ratio. Thus,  $\overline{N_{p.e.}}$  for 1 GeV photons is estimated to be 4200 photo-electrons, and the relative fluctuation is expected to be  $b' = 1/\sqrt{4200} = 1.5\%$ . The overall energy resolution for 1 GeV photons would be  $\sigma_E/E = \sqrt{a^2 + b^2 + b'^2} = 5.4\%$ , which means the energy resolution is dominated by the sampling fluctuation: the parameter  $b$ .

For the energy resolution of the upstream part,  $E_\gamma$  dependence is more complicated. The fraction of the energy deposit in the upstream part relatively reduces as  $E_\gamma$  increases because the position of shower maximum moves toward the downstream part. As a result, the energy resolution is deteriorated at high energy region ( $E_\gamma > 1$  GeV) due to the shower-leakage effect. At low energy, the contribution of the sampling fluctuation is still dominant, and hence the resolution improves with  $E_\gamma$ .

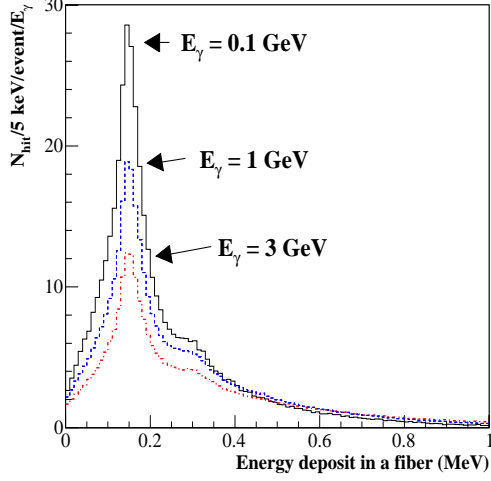


Figure 6: Distributions of energy deposit in a fiber for different energies.

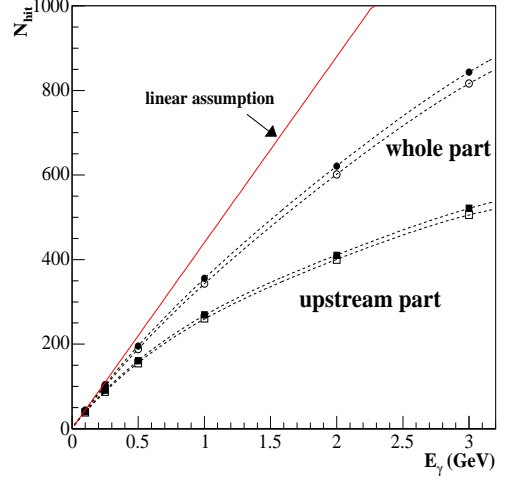


Figure 7: Energy dependence of the number of fiber hits for  $N_{p.e.} \geq 1$  (filled plots) and  $N_{p.e.} \geq 2$  (open plots).

### $E_\gamma$ dependence of the number of fiber-hits ( $N_{hit}$ )

Figure 6 shows the distributions of the energy deposit in a fiber for different incident energies, where the number of fiber-hits ( $N_{hit}$ ) is normalized by  $E_\gamma$ . The shape of distributions is independent of  $E_\gamma$ , where the sharp peaks at around 150 keV is the minimum ionization peak (MIP) due to a charged particle ( $e^-$  or  $e^+$ ) passing through a fiber. The result indicates that the information of  $E_\gamma$  is digitized by the number of fiber-hits, and hence one can estimate the photon energy by just counting the  $N_{hit}$ .

The incident-energy dependence of  $N_{hit}$  is shown in Fig.7, where the average number of photoelectrons is assumed to be 40 p.e./MeV. Although the relation between  $N_{hit}$  and  $E_\gamma$  is not linear, it shows one-to-one correspondence. The saturation effect is attributed that the number of fibers around the shower-maximum region is limited. Shower profile images of fibers having  $N_{p.e.} \geq 1$  are shown from Fig.8 to Fig.10 for  $E_\gamma = 1, 0.1$  and 3 GeV, respectively.

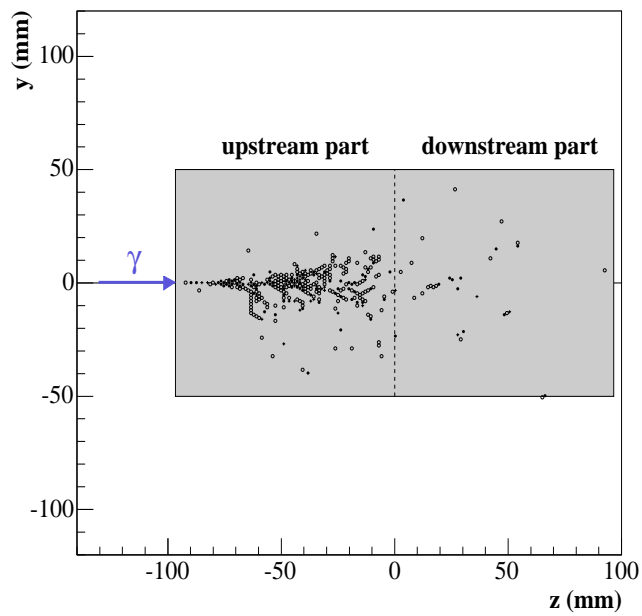
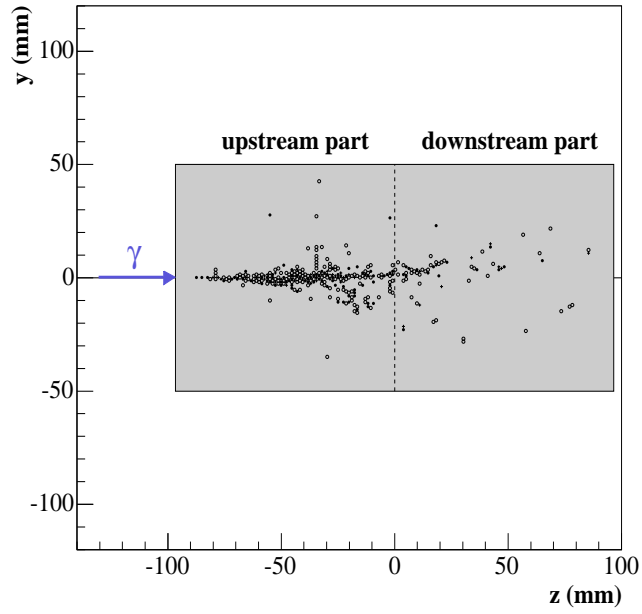


Figure 8: Two dimensional images of the fiber hits for  $E_\gamma = 1$  GeV.

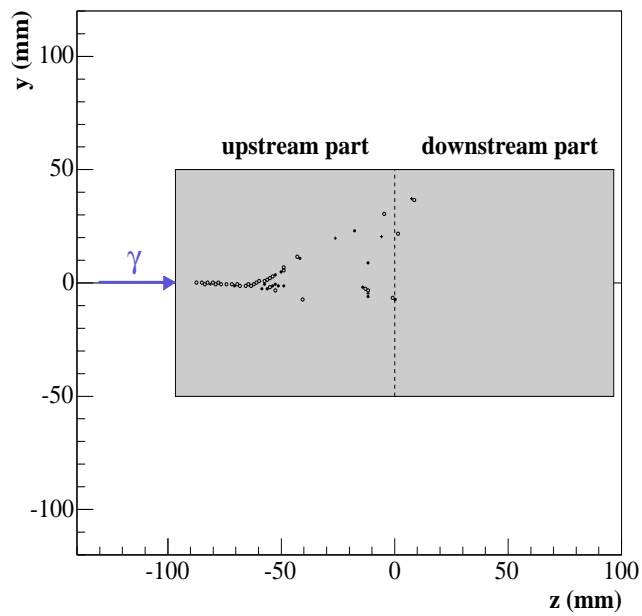
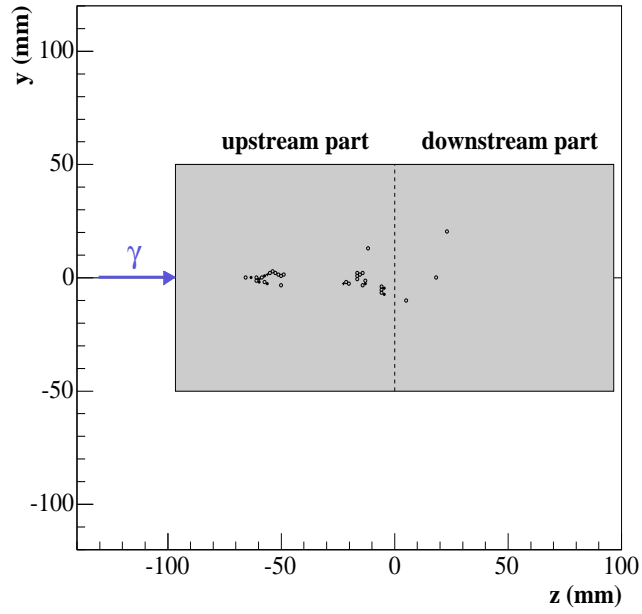


Figure 9: Two dimensional images of the fiber hits for  $E_\gamma = 0.1$  GeV.

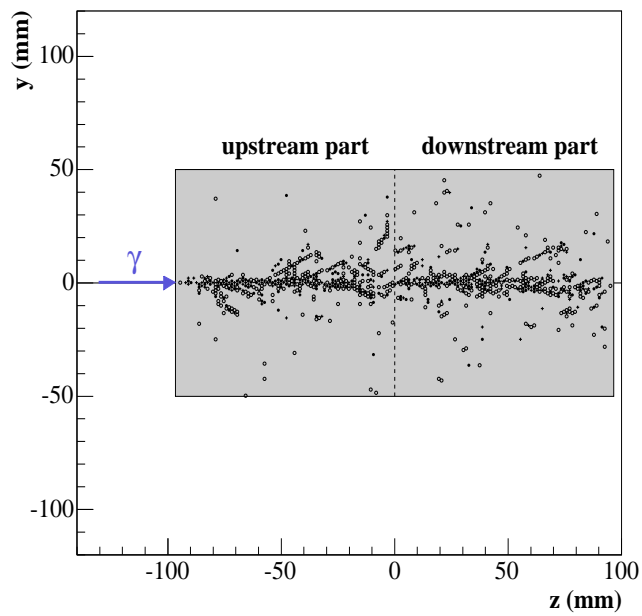
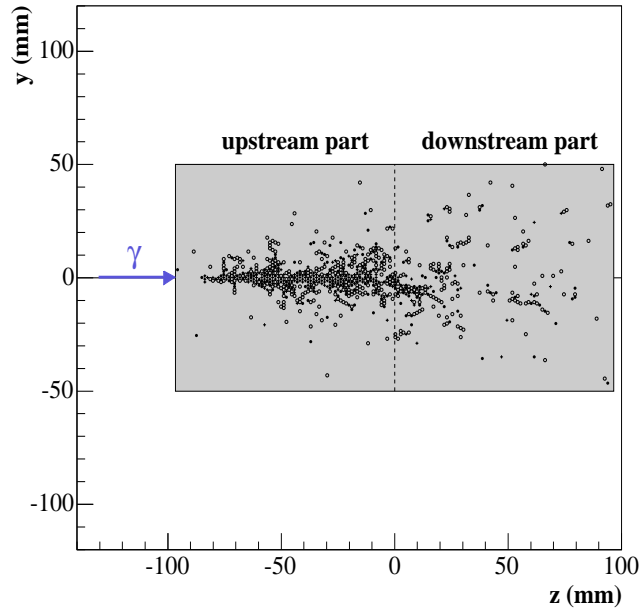


Figure 10: Two dimensional images of the fiber hits for  $E_\gamma = 3$  GeV.

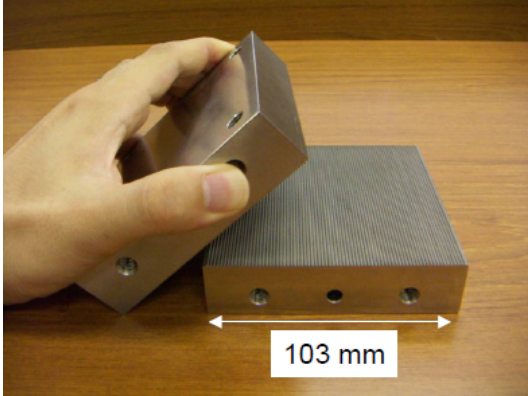


Figure 11: Metal mold for lead-sheet fabrication.

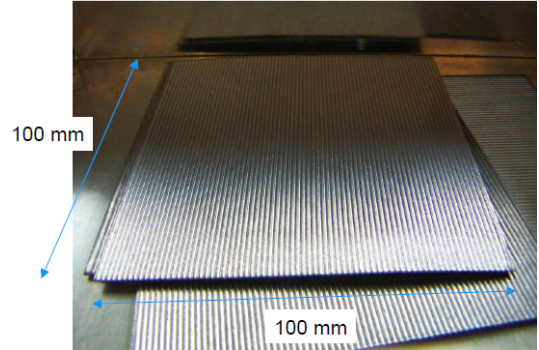


Figure 12: Samples of grooved lead sheet.

## 2.4 Construction

Construction of the prototype module was performed at NDA. The procedure can be summarized as following:

1. Grooved lead sheets fabrication
2. Alignment of 75 pieces of the fibers on a lead sheet
3. Gluing the fibers and lead with epoxy

The grooved lead sheets were shaped by pressing a sheet of pure lead ( $110 \times 110 \times 0.5$  mm) with a stainless-steel mold and a pressing machine. The mold, which had the area of  $103 \times 103$  mm<sup>2</sup>, was made by using the wire-spark erosion method (Fig.11). To ensure the proper shaping, we pressed the lead sheet with the pressure of 350 kgw/cm<sup>2</sup>. The problem was that the pressed lead sheet was stuck to the metal mold, and the sheet tore when one peeled it from the mold. We solved it by inserting two sheets of vinyl sheet (30  $\mu$ m) at both faces of a lead sheet. A picture of the grooved lead sheet is shown in Fig.12 .

After the fabrication of the grooved lead sheets, we aligned the 75 pieces of scintillating fiber on the sheet (Fig.13). For gluing between fibers and lead sheets we used a low-viscosity epoxy-glue (CLEAR COAT produced by SYSTEMTHREE), where the set-time of the epoxy is 9 hours at 25°C. We repeated the layer stacking in this way. Figure 14 shows a 10-layers sample-module.



Figure 13: Picture of layer stacking.

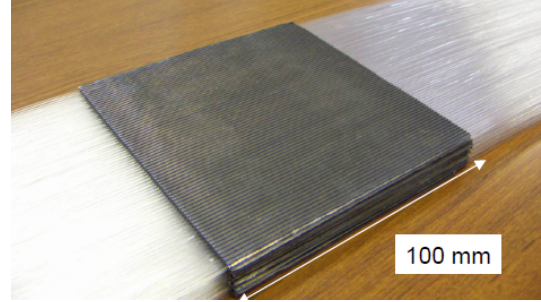


Figure 14: Sample module of 10 fiber layers.

### 3 Proposed Experiment

#### 3.1 General description of the experiment

The main purpose of the experiment is to check the performance of a prototype spaghetti-calorimeter module with the bremsstrahlung photons ( $E_\gamma = 0 \sim 8$  GeV) at LEPS beam-line. Following items will be tested in the experiment:

- reconstruction efficiency of the shower profile
- energy resolution
- position and angular resolutions for different angle of incidence

Performance of the prototype module evaluated by the experiment will be utilized in a Monte-Carlo simulation for larger and more complex calorimeter system. Therefore, this experiment is very important to design suitable experimental setup for the J-PARC experiment.

The prototype module will be placed just before the TOF wall in the experimental hatch. The bremsstrahlung photons generated from the straight section in the storage ring are injected onto the module surface.

#### 3.2 Beam condition

In order to collect the light from the phosphor screen of IIT-1 effectively, the gate width for the IIT-2 has to be set about  $100 \mu\text{sec}$ . In this case, the most serious problem would be the pile-up effect in the image. If two photons hit on the module during the gate width, the two images produced by the photons are overlapped and these are not distinguishable. Therefore, the

intensity of the photon beam has to be as low as possible in order to avoid the pile-up effect. For this reason, we need a collimator having a diameter of less than 1 mm $\phi$  at before the sweeping magnet in the laser hatch.

Both the intensity and the size of the bremsstrahlung photon at the laser hatch were measured with a PWO detector in 1999. At that time, we obtained following results:

- beam intensity at storage current 100 mA ( $> 1$  GeV):  $\sim 50$  kcps
- beam size at the behind of the sweep magnet: 3.6 mm (horizontal), 2.2 mm (vertical)

Note that the collimator size was 20 mm $\phi$  in the measurement. Although the storage ring parameters, such as  $\beta$  function, and vacuum pressure in the straight section might be changed at the present time, we estimated the beam intensities with 1 mm $\phi$  and 0.5 mm $\phi$  collimator using these values; they are summarized as following:

- beam intensity with 1.0 mm $\phi$  collimator ( $> 10$  MeV): 2.6 kcps
- beam intensity with 0.5 mm $\phi$  collimator ( $> 10$  MeV): 0.6 kcps

where we assumed that the beam-size distribution has a simply Gaussian form, the  $E_\gamma$  dependence of the cross section for the bremsstrahlung photons shows  $1/E_\gamma$  and the prototype module is sensitive to the  $E_\gamma > 10$  MeV photons. The probabilities of the pile-up with gate width of 100  $\mu$ sec would be 40% for 1 mm $\phi$  and 11% for 0.5 mm $\phi$ , respectively. For further reduction of the pile-up events we will record the wave form of the PMT signals with an FADC module; it makes us to remove these events at off-line level.

### 3.3 Data Acquisition

An illustration of the circuit scheme is shown in Fig.15. The summed signals from both upstream and downstream PMTs are discriminated; then the generated logic signals will be thinned out to be  $\sim 20$  Hz to make trigger signals. The analog signals from each PMT are collected by a charge sensitive ADC (CS-ADC) for photon-energy measurement.

Analog-video signals from the CCD camera are sent to a 8bit FADC, where the pixel signals that exceed some threshold are digitized. The 8bit digital data are stored to the VME FIFO-module, which has the 32k FIFO memory of the 32bit data, in synchronization with the pixel clock generated by the clock and coordinate generator (CCG). The 10bits data which is the pixel-position information for the X and Y coordinate are also recorded to the FIFO module at the same time.

For absolute energy calibration we collect timing signals of the tagging-scintillator hodoscope, which consists of 10 scintillators located just after the bending magnet in the storage ring. The

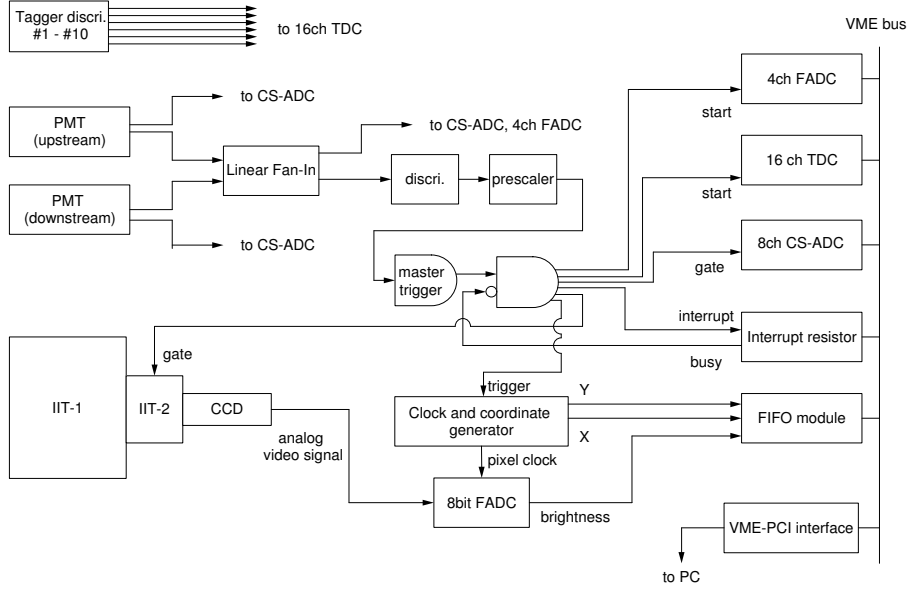


Figure 15: Circuit scheme of the experiment.

energy acceptance of the hodoscope ranges from  $E_\gamma = 1.5$  GeV to  $E_\gamma = 3.5$  GeV and the energy interval of each scintillator is about 200 MeV.

All data stored in the VME modules are sent to a PC-Linux machine via the VME-PCI interface (SBS model 620) event by event.

### 3.4 Data statistics

We will tune the trigger rate to be 20 Hz for photons whose energy is more than 10 MeV. Hence, 72000 events are collected with 1 hour data-taking by assuming DAQ live-time is nearly 100%. In these events 40% of events will be removed in the off-line analysis to reject the pile-up image, if we install a 1 mm $\phi$  collimator. Thus, total events which can be analyzed are expected to be 43000 events for photons with  $100 \text{ MeV} < E_\gamma < 8 \text{ GeV}$ . The number of events having a signal from the tagger hodoscope covering the highest energy region ( $3.3 \sim 3.5$  GeV) is estimated to be  $\sim 600$  events in this case. Therefore, at least, we need 17 hours data-taking in order to check the linearity of the pulse height within 1% accuracy.

We also planning to take data for different angle of incidence. Thus, we request 4 days for data taking.

## 4 Conclusion and Requests

To study the performance of the spaghetti calorimeter, we request 1 day for detector setup, 2 days for tuning of circuit and collimator position and 4 days for data taking.

We will use the bremsstrahlung photons produced at the straight section; thus, no laser is necessary. No materials are required in the beam line except for the absorber for synchrotron radiation (Pb 1.5 mm) and drift chambers.

Timing signals of the tagger hodoscope are necessary for linearity check and absolute energy calibration.

Special request is the installation of a collimator ( $< 1 \text{ mm}\phi$ ) just before the sweep magnet in the laser hatch.

## References

- [1] Y. B. Hsiung *et al.* Letter of intent for Nuclear and Particle Physics Experiments at J-PARC (L05)
- [2] V. N. Ivanchenko *et al.* Nucl. Instr. Meth. A494, 514 (2000)